

Data Fusion Modelling of Visible-near-infrared and Mid-infrared Spectra

S. Hamed Javadi^a and Abdul M. Mouazen^{a,*}

^a Precision Soil and Crop Engineering Group, Faculty of Bioscience Engineering, Ghent University, Gent, Belgium.

* Corresponding author. Email: Abdul.mouazen@ugent.be

Abstract

Spectroscopy has emerged as a solution to estimate key soil attributes in precision agriculture (PA) during recent decades. Chemometrics and machine-learning methods are used in order to extract useful information out of the spectra. In this paper, the performance of visible-near-infrared (Vis-NIR) and mid-infrared (MIR) spectrophotometers for the prediction of pH, organic carbon (OC), phosphorous (P), potassium (K), magnesium (Mg), calcium (Ca), sodium (Na), moisture content (MC), and cation exchange capacity (CEC) were evaluated. Using 267 soil samples measured with a CompactSens spectrometer (tec5 technology, Germany) with 350-1700nm spectral range and a 4300-FTIR (Agilent, US) with 650-4000cm⁻¹ spectral range, we compared single-sensor partial least squares (PLS) regression after feature selection. To take advantage of both sensors, the combined use of them were evaluated in three fusion scenarios: 1. Spectral concatenation (SC) in which the raw vis-NIR and MIR spectra are concatenated; 2. Feature fusion (FF) wherein the features (i.e., selected spectral ranges) of vis-NIR and MIR are concatenated; and 3. Fusion of the predictions given by vis-NIR and MIR PLS-based models by linear regression (LR). The validation results showed that the vis-NIR model outperforms the MIR model in the prediction of all studied attributes, except for pH, Ca, and CEC. Furthermore, the single-sensor accuracies were improved in all cases by LR while SC and FF enhanced the single-sensor accuracies just in cases of OC, Ca, and CEC with FF being superior to SC. However, the improvement achieved by fusion was not significant. Accordingly, it is suggested to use just vis-NIR for prediction of the studied soil attributes since it showed more robustness than MIR.

Keywords: Data fusion; precision agriculture; spectroscopy; visible-near-infrared; mid-infrared.

1. Introduction

Precision agriculture (PA) has emerged as a sustainable and profitable solution (Mouazen et al., 2019). In PA practices, it is essential to identify variability within the field by assessing soil properties for which spectroscopy is a fast and inexpensive method (Ben-Dor and Banin, 1994; Guzmán Q. et al., 2018; Stenberg et al., 2010). Different kinds of spectrometers, including visible-near-infrared (vis-NIR), mid-infrared (MIR), and X-ray fluorescence (XRF), are being used for this purpose, each potentially providing information about different soil attributes. Accordingly, the potential of single-sensor and combined use of these devices in prediction of different soil fertility attributes needs to be evaluated. While single-sensor of each of these spectroscopy sensors were studied intensively, the fusion of their output is still in its early stage of research. A common hypothesis is that the fusion data of multiple sensors can improve the overall prediction accuracy, compare to the single-sensor solution. However, it has been shown in (Javadi et al., 2021; Javadi and Mouazen, 2021; Tavares et al., 2021) that this cannot always be the case when using vis-NIR and XRF, as there might be no synergy between vis-NIR and XRF data.

While there is an extensive literature on soil analysis by vis-NIR (Chabrilat et al., 2019; Fidêncio et al., 2002; Kodaira and Shibusawa, 2020; Mouazen et al., 2005; Mouazen and Kuang, 2016; Shepherd and Walsh, 2002), a review of soil analysis with a focus on MIR has been provided by (Janik et al., 1998). Normally, machine-learning-based algorithms are exploited in order to predict the soil attributes out of the vis-NIR and MIR spectra. Mostly, instead of using all the reflectance values all over the whole spectral ranges, the relevant latent variables are used since the high-dimensional spectra are highly correlated. To this end, either principal components regression (Chang et al., 2001) or partial least squares (PLS) regression (Javadi et al., 2021; Javadi and Mouazen, 2021; Tavares et al., 2021) are used. The PLS model is more advantages since it considers covariance maximization between the latent variables of the predictors and the predicted values. Nevertheless, both vis-NIR and MIR sensors have shown limited performance in soil analysis and the potential in combined use of them needs to be studied using different types of soil and in different prediction methodologies.

In this paper, we studied potential of the vis-NIR and MIR spectra in prediction of key soil fertility attributes including pH, organic carbon (OC), phosphorous (P), potassium (K), calcium (Ca), magnesium (Mg), moisture content (MC), sodium (Na), and cation exchange capacity (CEC). Especially, we used the PLS-based prediction model and incorporated feature selection based on the regression coefficients in order to make the models simpler and more efficient. This also facilitates studying the potential synergy between the two spectral kinds. Furthermore, three fusion schemes were evaluated including low-level fusion, feature fusion, and high-level fusion. In the low-level fusion scheme – spectra concatenation (SC), the raw spectra are concatenated to each other forming a single spectrum which covers vis-NIR and MIR spectral ranges. In the feature fusion (FF) scheme, the selected spectral ranges of vis-NIR and MIR are concatenated and subjected to a PLS model. Finally, in the high-level fusion, the predictions given by the single-sensor PLS-based models are fused according to linear regression (LR).

2. Materials and Methods

2.1. Study sites and soil sampling

In this study, we used totally 267 soil samples from different locations of nine fields in Flanders, Belgium. The soil samples were collected at 10-20 cm soil depth, with an average spatial sampling rate of 3.25 samples/ha during 2018. The fields included Bottelare (5ha), Thierry (3ha), Watermachine (6ha), Beers (12ha), Kouter (13ha), Gingelomse (11ha), Dal (6ha), Kattestraat (5ha), and Grootland (21ha). The information of the study fields has been provided in Table 1. Topographically, the Gingelomse and Bottelare fields had mild undulations but other fields' surfaces were rather flat. Also, there was a high percentage of salt (Ca^{++}) in the soil of Watermachine and Beers located close to North Sea. Across all fields, a general cropping rotation of maize, potato, sugar beets, and barley/wheat is being performed with an intermittent short duration cover crop.

Table 1. The information of the study fields in different areas of Flanders in Belgium.

Field name	Location	Date of sampling (2018)	No. of Samples	Crop Type	Soil Texture	Average MC* (%)	Average OC** (%)
Bottelare	Melle	Nov.	23	Maize	Silt Loam	14.64	1.60
Thierry	Moeskroen	Aug.	13	Wheat	N.A.*	15.56	1.66
Watermachine	Veurne	Aug.	19	Wheat	Loam	19.86	1.35
Beers	Veurne	Aug.	38	Oil seed rape	Sandy Loam	19.30	1.29
Kouter	Huldenberg	Jul./Aug.	40	Burley	Silt Loam	3.63	1.10
Gingelomse	Landen	Dec.	37	Barley	Silt Loam	22.79	1.34
Dal	Landen	Dec.	21	Sugar beet	N.A.	23.02	1.38
Kattestraat	Landen	Aug.	19	Barley	N.A.	8.75	1.47

* N.A.: not available

2.2. Laboratory soil measurement

Each soil sample was reduced to 400g following standard coning and quartering methods [29]. Each fresh sample was mixed well and stones/gravels, grass, and stubble, were removed. Then, it was divided into two parts of 200g each. One part was used for optical measurements in laboratory while the chemical analysis was performed on the other part. For optical measurements, samples were air-dried for more than two weeks, then they were crushed using an agate mortar and pestle and then they were sieved using a 2mm stainless steel sieve.

2.3. Measurement by visible and near infrared (vis-NIR) and mid-infrared (MIR) spectrometers

We placed about 50g of each dried and sieved soil sample into three Petri dishes (diameter = 2cm and depth = 1cm). In order to ensure maximum diffuse reflection and increase signal-to-noise ratio [30], each soil sample was gently pressed and levelled using a spatula. We scanned the Soil samples using a CompactSpec vis-NIR spectrophotometer (Tec5 Technology for spectroscopy, Germany) in diffuse reflectance mode, with wavelength range of 305 - 1700nm. A 100% reflectance ceramic disc was scanned or the device calibration every 30 minutes. Ten spectra per Petri dish were collected and the resultant 30 spectra per three dishes were averaged in one spectrum per sample.

The soil samples were then scanned using an Agilent 4300 handheld Fourier transfer infrared (FTIR) spectrometer (Agilent Technologies, Santa Clara, CA, United States), with a spectral wavenumber range of 4000 cm^{-1} to 650 cm^{-1} with 8 cm^{-1} resolution. The background spectrum was taken out using a silver-plated reference cap provided by the manufacturer every 30 min during scanning. The background scan provides a baseline profile of the system conditions with no sample loaded on the instrument, and helps to correct for changes in the environment (e.g., changes in local atmospheric composition) influencing measurement as well as potential instrument drift. The spectral data were collected as absorbance using the Microlab software V5.0 provided by the manufacturer together with the spectrometer. Average absorbance of the three scans was used for spectra pre-treatment and model establishment.

2.4. Chemical analysis in laboratory

The other half part of each soil sample dedicated for the laboratory chemical analysis was kept at $4\text{ }^{\circ}\text{C}$ within a cooling room and then was given to the Soil Survey of Belgium (BDB, Heverlee, Belgium) for chemical analysis of soil OC, pH, Ca, and Mg. OC was obtained using the dry combustion following Dumas principle (ISO 10694; CMA/2/II/A.7; BOC). Before OC measurement, total inorganic carbon compounds were removed by treating the soil samples with hydrochloric (HCl) acid. Soil pH, after shaking and equilibrium for 2h in mol/l potassium chloride solution (KCl), was measured in the supernatant, using 1:2.5 soil to solution ratio. The available Mg and Ca were determined in ammonium lactate extract with inductively coupled plasma atomic emission spectroscopy (ISO 11885; CMA 2 / I / B1). Table 2 has listed the statistics of the laboratory measured soil attributes for the soil samples of each field.

Table 2. The results of the laboratory measured soil organic carbon (OC), pH, magnesium (Mg), calcium (Ca), phosphorous (P), potassium (K), sodium (Na), moisture content (MC), and cation exchange capacity (CEC).

	pH	OC (%)	P (mg/100g)	K (mg/100g)	Mg (mg/100g)	Ca (mg/100g)	Na (mg/100g)	MC (%)	CEC (%)
mean	6.93	1.31	27.2	30.02	27.85	597.53	5.76	16.45	33.22
Standard deviation	0.58	0.28	9.47	11.03	19.85	794.09	4.58	6.77	40.95
Minimum	5	0.77	8	10	7	83	0.94	2.28	5.92
maximum	8	2.4	69	69	85	4210	30	28.81	215.09

2.5. Single-sensor modelling

Out of the 267 soil samples, 13 samples were detected as outliers using the Mahalanobis distance criterion (De Maesschalck et al., 2000). Using Kennard-Stone algorithm (Nawar and Mouazen, 2018), the whole dataset was divided into calibration and validation sets of 200 and 55 samples each, respectively.

The PLS model was adopted for predicting the soil attributes using single sensors. The number of the latent variables was optimized for each soil attribute according to the leave-one-out cross-validation results. Then, the optimal wavelength ranges for vis-NIR and MIR, respectively were obtained by grid search through all the regression coefficients with the RMSE of the leave-one-out cross-validation as the objective. More specifically, the regression coefficients were sorted first. Then, in each step, the variables with coefficients more than a threshold were used for cross-validation. The set of the variables giving the minimum RMSE was selected and used for calibrating the prediction models. After having the model calibrated, it was validated using the soil samples of the validation set.

2.6. Fusion models

Three fusion schemes (shown in Figure 1) were evaluated which are discussed in the following.

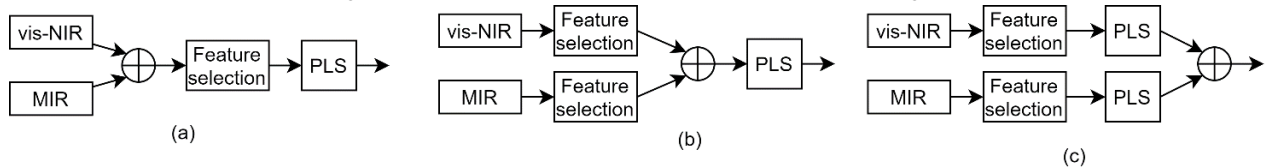


Figure 1. Studied schemes for fusion of visible-near-infrared (vis-NIR) and mid-infrared (MIR) spectra using partial least squares (PLS) modelling. (a) spectra concatenation (SC); (b) Feature fusion (FF); (c) Fusion of the single-sensor predictions based on linear regression (LR).

2.6.1. Spectra concatenation (SC)

In this scheme (Figure 1-a), the vis-NIR and MIR spectra are concatenated to each other to form a single spectrum covering the vis-NIR and MIR spectral range. Note that the spectral range between 1650 nm to 2550 nm was not covered due to limitation of the devices used and also due to edge cutting of the spectra in preprocessing. The concatenated spectrum is treated the same as a single spectrum and the same procedure as the vis-NIR and MIR modelling is applied on it. More specifically, the optimal number of latent variables is obtained according to the cross-validation results. Then, the optimal features (i.e., the optimal wavelength ranges) are obtained based on which the PLS model is established. SC has been examined in several works (Javadi et al., 2021; Tavares et al., 2021) but here we applied feature selection on the concatenated spectra rather than applying the raw concatenated spectra directly to the prediction model.

2.6.2. Feature fusion (FF)

Feature fusion (FF) – shown in Figure 1-b – is based on concatenating the selected spectral ranges of vis-NIR and MIR spectra to each other. FF is based on the fact that instead of fusing the raw data, as in SC, their features which are more informative can be used. This simplifies the fusion prediction model as well.

2.6.3. Linear regression (LR)

The highest level of fusion includes just the predictions given by the single-sensor models. The method – referred to as model averaging (O'Rourke et al., 2016) and Granger-Ramanathan (GR) (Granger and Ramanathan, 1984; Xu et al., 2019) as well – gives the final prediction of the soil attributes based on linear regression (LR) of the single-sensor predictions. We tag this fusion scheme by LR in order to highlight the prediction method used, i.e., LR. LR is simply a weighted sum of the single-sensor predictions with the more accurate single-sensor prediction weighed more.

2.7. Evaluation criteria

The prediction accuracies of the above listed individual and fusion models were evaluated in terms of root mean square error (RMSE), ratio of performance to deviation (RPD), and Lin's concordance correlation coefficient (LCCC). RPD is defined as the ratio of the standard deviation of the measured soil property divided by the RMSE of the prediction. LCCC is a measure of concordance between new measurements, y , and the reference values, r , and is given by (Lin, 1989):

$$LCCC = \frac{2\rho\sigma_y\sigma_r}{\sigma_y^2 + \sigma_r^2 + (\bar{y} - \bar{r})^2} \quad (1)$$

wherein σ_y and σ_r denote the standard deviation of the measurements and the reference values, respectively, and ρ is the related Pearson correlation coefficient. Indeed, LCCC modifies the Pearson correlation coefficient by measuring how far the best-fit line is from the 45-degree line through the origin in addition to assessing the closeness of the data to the best-fit line.

3. Results and Discussion

The selected spectral ranges and spectral bands for the single-sensor models and also for SC are shown in Figure 2, Figure 3, and Figure 4. OC and MC have spectra responses in NIR spectra. As shown in Figure 2, the optimal wavelength ranges of OC and MC include their corresponding range in vicinity of 1000 nm and 1400 nm, respectively (Chabrilat et al., 2019). The other soil attributes do not have direct impact on the spectral data but can still be estimated with vis-NIR spectroscopy, as they are known to be correlated with properties have direct spectral responses in the NIR range.

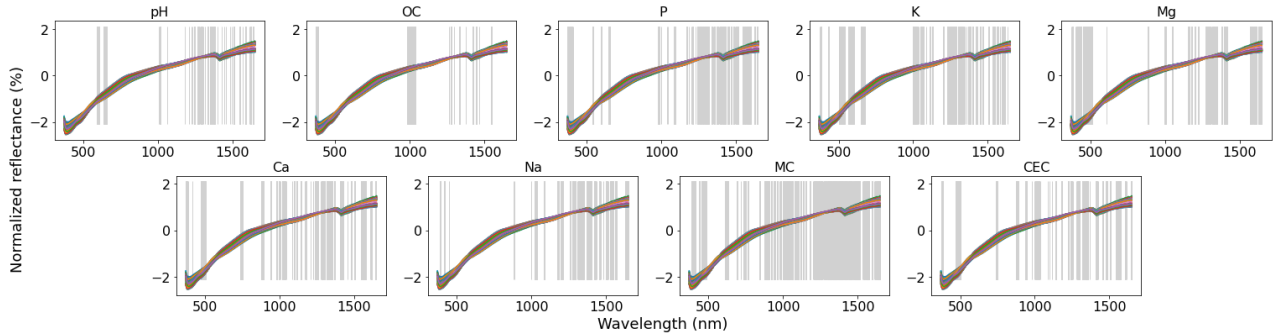


Figure 2. The normalized visible-near-infrared (vis-NIR) spectra and their selected spectral ranges for studied soil attributes. OC: organic carbon; P: phosphorous; K: potassium; Mg: magnesium; Ca: calcium; Na: sodium; MC: moisture content; CEC: cation exchange capacity.

In the MIR selected features (Figure 3) for the OC prediction model include its important range in vicinity of 3200 nm (Cañasveras Sánchez et al., 2012). For other soil attributes, also the optimal spectral ranges have been used, especially for Ca which include the range in vicinity of 4000 nm. The selected features of vis-NIR and MIR (Figure 4) were concatenated and subjected to a PLS-based model in the FF scheme. On the other hand, in SC, the optimal wavelength ranges are selected from the whole concatenated spectra.

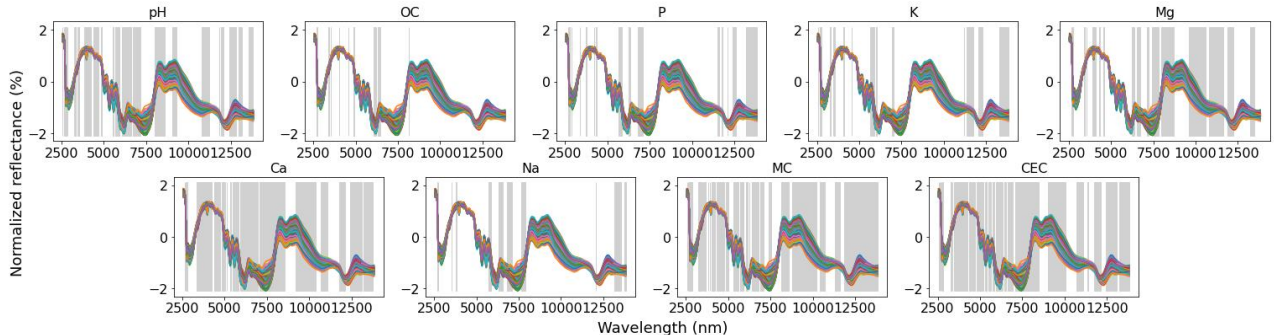


Figure 3. The normalized mid-infrared (MIR) spectra and their selected spectral ranges for studied soil attributes. OC: organic carbon; P: phosphorous; K: potassium; Mg: magnesium; Ca: calcium; Na: sodium; MC: moisture content; CEC: cation exchange capacity.

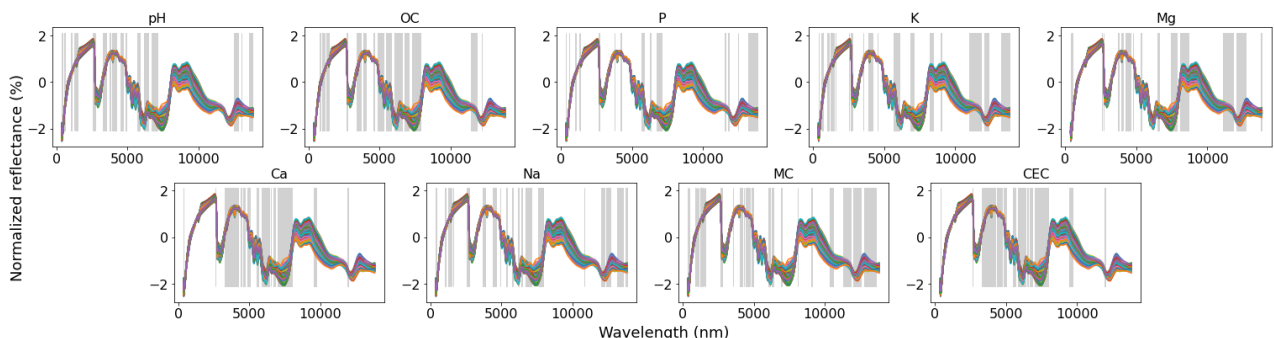


Figure 4. The normalized concatenated visible-near-infrared (vis-NIR) and mid-infrared (MIR) spectra and their selected spectral ranges in the spectra concatenation (SC) scheme for predicting the studied soil attributes. OC: organic carbon; P: phosphorous; K: potassium; Mg: magnesium; Ca: calcium; Na: sodium; MC: moisture content; CEC: cation exchange capacity.

The performance of the single-sensor and the fusion models is shown in Figure 5 in terms of RPD and LCCC. Also, the RMSE values of the models are listed in Table 3. Comparing the single-sensor models shows that MIR outperforms vis-NIR just in prediction of pH, Ca, and CEC while the vis-NIR performance is also acceptable in all these cases. As can be seen, fusion was effective in all cases, especially with regard to LR and FF. LR outperformed the single-sensor accuracies for all soil attributes. With FF and SC, the predictions were improved in OC, Ca, and CEC wherein FF outperformed SC which indicates that the features selected in single-sensor models expose synergy. All single-sensor and fusion models gave excellent performance ($RPD \geq 2$) in pH, Mg, Ca, and CEC. However, the LCCC value for all models are more than 0.4, which indicates an appropriate response of all models, even in cases of P, K, and Na whose RPD might not seem acceptable ($RPD < 2$). It is worth mentioning, as has also been pointed out in (Javadi and Mouazen, 2021; Tavares et al., 2021), that when a single device performs satisfactorily, its fusion with a poorly-behaving sensor may degrade the performance. A good example of this is the MC case where vis-NIR model gave an excellent accuracy while its fusion with the MIR model degraded the accuracy in FF and SC fusion schemes; though the overall performance was more enhanced using LR. Note that the LR performance was just slightly better than the best single-sensor model in cases where SC and FF were not able to enhance the overall accuracy (cf. Table 3). Accordingly, it can be concluded that each of the vis-NIR and MIR spectra are not capable of complementing each other for all soil properties investigated, so their combined use for all properties except Ca and CEC is not advantageous, as also pointed out by (Rossel et al., 2006).

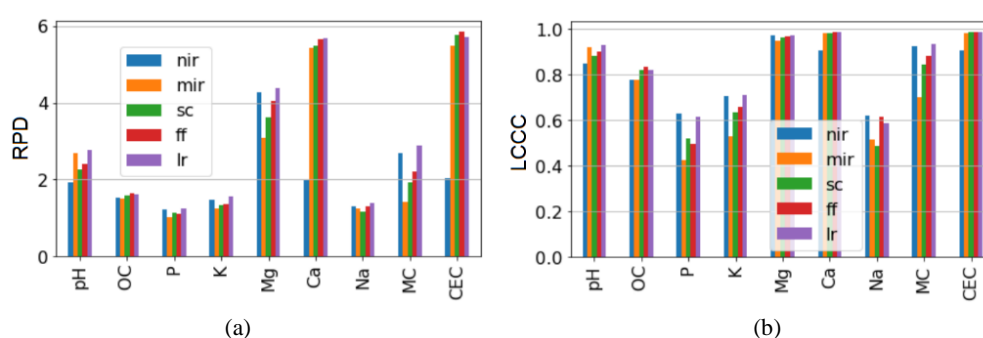


Figure 5. The (a) ratio of performance to deviation (RPD) and (b) Lin's concordance correlation coefficient (LCCC) of single-sensor modelling of visible-near-infrared (NIR), mid-infrared (MIR), and the studied three fusion scheme including spectra concatenation (SC), feature fusion (FF), and linear regression (LR). OC: organic carbon; P: phosphorous; K: potassium; Mg: magnesium; Ca: calcium; Na: sodium; MC: moisture content; CEC: cation exchange capacity.

Table 3. The root mean squared error (RMSE) of single-sensor modelling of visible-near-infrared (NIR), mid-infrared (MIR), and the studied three fusion scheme including spectra concatenation (SC), feature fusion (FF), and linear regression (LR). OC: organic carbon; P: phosphorous; K: potassium; Mg: magnesium; Ca: calcium; Na: sodium; MC: moisture content; CEC: cation exchange capacity.

	vis-NIR	MIR	SC	FF	LR
pH	0.25	0.18	0.21	0.2	0.18
OC (%)	0.15	0.15	0.14	0.14	0.14
P (mg/100g)	6.45	7.78	7.06	7.19	6.42
K (mg/100g)	7.6	8.91	8.37	8.15	7.21
Mg (mg/100g)	3.73	5.16	4.39	3.95	3.67
Ca (mg/100g)	273.44	99.82	98.78	95.85	96.19
Na (mg/100g)	3.27	3.38	3.67	3.3	3.12
MC (%)	2.41	4.55	3.33	2.92	2.25
CEC (mg/100g)	13.82	5.12	4.88	4.82	4.99

4. Conclusions

In this paper, the potential of vis-NIR and MIR and their combined use in prediction of key soil fertility attributes [e.g., pH, OC, P, K, Ca, Mg, Na, MC, and CEC] were studied. Notably, optimal wavelength ranges of the vis-NIR and MIR spectra were obtained by cross-validation through the regression coefficients. More specifically, those spectral ranges with significant regression coefficient that gave the best PLS-based cross-validation results were used while the other ranges were neglected. Furthermore, three fusion schemes were assessed: 1. Spectra concatenation (SC) in which the whole vis-NIR and MIR spectra are concatenated after feature selection (based on regression coefficient – similar to single-sensor modelling), and are subjected to a PLS model; 2. Feature fusion (FF) which concatenates the selected

spectral ranges of the vis-NIR and MIR spectra and subjects it to a PLS model; and 3. Fusing the single-sensor prediction by linear regression (LR). The validation results showed that all single-sensor and fusion models performs satisfactorily in prediction of pH, Mg, Ca, and CEC. Comparing the single-sensor models showed the superiority of vis-NIR in all cases except for pH, Ca, and CEC wherein its performance was also acceptable with $RPD \geq 1.98$. While LR was effective in enhancing the single-sensor accuracies, SC and FF were successful just in cases of OC, Ca, and CEC wherein FF outperformed SC. However, we noted that the improvement achieved by fusion was not significant. Accordingly, the information provided by the vis-NIR spectra did not complement that of the MIR spectra and just vis-NIR would be sufficient for prediction of the studied soil attributes since it exhibited more robustness than MIR. As future directions, it is suggested to examine the studied models with a wider range vis-NIR spectrometers and detector types. Moreover, feature selection was done here based on the regression coefficient since a linear prediction model (i.e., PLS) was adopted. Feature selection by an evolutionary algorithm – e.g., the genetic algorithm (GA) – together with a nonlinear prediction model – such as random forest or artificial neural network – can be considered as a future study topic.

Acknowledgements

Authors acknowledge the financial support received from the European Commission for SIEUSOIL project (No. 818346).

References

- Ben-Dor, E., Banin, A., 1994. Visible and near-infrared (0.4–1.1 μm) analysis of arid and semiarid soils. *Remote Sens. Environ.* 48, 261–274. [https://doi.org/https://doi.org/10.1016/0034-4257\(94\)90001-9](https://doi.org/https://doi.org/10.1016/0034-4257(94)90001-9)
- Cañasveras Sánchez, J.C., Barrón, V., del Campillo, M.C., Viscarra Rossel, R.A., 2012. Reflectance spectroscopy: a tool for predicting soil properties related to the incidence of Fe chlorosis. *Spanish J. Agric. Res.* Vol 10, No 4 (2012)DO - 10.5424/sjar/2012104-681-11 .
- Chabrilat, S., Ben-Dor, E., Cierniewski, J., Gomez, C., Schmid, T., van Wesemael, B., 2019. Imaging Spectroscopy for Soil Mapping and Monitoring. *Surv. Geophys.* 40, 361–399. <https://doi.org/10.1007/s10712-019-09524-0>
- Chang, C.-W., Laird, D.A., Mausbach, M.J., Hurburgh, C.R., 2001. Near-Infrared Reflectance Spectroscopy–Principal Components Regression Analyses of Soil Properties. *Soil Sci. Soc. Am. J.* 65, 480–490. <https://doi.org/10.2136/sssaj2001.652480x>
- De Maesschalck, R., Jouan-Rimbaud, D., Massart, D.L., 2000. The Mahalanobis distance. *Chemom. Intell. Lab. Syst.* 50, 1–18. [https://doi.org/https://doi.org/10.1016/S0169-7439\(99\)00047-7](https://doi.org/https://doi.org/10.1016/S0169-7439(99)00047-7)
- Fidêncio, P.H., Poppi, R.J., de Andrade, J.C., 2002. Determination of organic matter in soils using radial basis function networks and near infrared spectroscopy. *Anal. Chim. Acta* 453, 125–134. [https://doi.org/https://doi.org/10.1016/S0003-2670\(01\)01506-9](https://doi.org/https://doi.org/10.1016/S0003-2670(01)01506-9)
- Granger, C.W.J., Ramanathan, R., 1984. Improved methods of combining forecasts. *J. Forecast.* 3, 197–204.
- Guzmán Q., J.A., Rivard, B., Sánchez-Azofeifa, G.A., 2018. Discrimination of liana and tree leaves from a Neotropical Dry Forest using visible-near infrared and longwave infrared reflectance spectra. *Remote Sens. Environ.* 219, 135–144. <https://doi.org/https://doi.org/10.1016/j.rse.2018.10.014>
- Janik, L.J., Merry, R.H., Skjemstad, J.O., 1998. Can mid infrared diffuse reflectance analysis replace soil extractions? *Aust. J. Exp. Agric.* 38, 681–696.
- Javadi, S.H., Mouazen, A.M., 2021. Data Fusion of XRF and Vis-NIR Using Outer Product Analysis, Granger–Ramanathan, and Least Squares for Prediction of Key Soil Attributes. *Remote Sens.* . <https://doi.org/10.3390/rs13112023>
- Javadi, S.H., Munnaf, M.A., Mouazen, A.M., 2021. Fusion of Vis-NIR and XRF spectra for estimation of key soil attributes. *Geoderma* 385, 114851. <https://doi.org/https://doi.org/10.1016/j.geoderma.2020.114851>
- Kodaira, M., Shibusawa, S., 2020. Mobile Proximal Sensing with Visible and Near Infrared Spectroscopy for Digital Soil Mapping. *Soil Syst.* . <https://doi.org/10.3390/soilsystems4030040>
- Lin, L.I.-K., 1989. A Concordance Correlation Coefficient to Evaluate Reproducibility. *Biometrics* 45, 255–268. <https://doi.org/10.2307/2532051>
- Mouazen, A.M., Alexandridis, T., Buddenbaum, H., Cohen, Y., Moshou, D., Mulla, D., Nawar, S., Sudduth, K.A., 2019. Monitoring, in: *Agricultural Internet of Things and Decision Support for Precision Smart Farming.* pp. 36–138.
- Mouazen, A.M., Kuang, B., 2016. On-line visible and near infrared spectroscopy for in-field phosphorous management. *Soil Tillage Res.* 155, 471–477. <https://doi.org/https://doi.org/10.1016/j.still.2015.04.003>
- Mouazen, A.M., Saeys, W., Xing, J., Baerdemaeker, J. De, Ramon, H., 2005. Near Infrared Spectroscopy for Agricultural Materials: An Instrument Comparison. *J. Near Infrared Spectrosc.* 13, 87–97. <https://doi.org/10.1255/jnirs.461>
- Nawar, S., Mouazen, A.M., 2018. Optimal sample selection for measurement of soil organic carbon using on-line vis-

- NIR spectroscopy. *Comput. Electron. Agric.* 151, 469–477. <https://doi.org/https://doi.org/10.1016/j.compag.2018.06.042>
- O'Rourke, S.M., Minasny, B., Holden, N.M., McBratney, A.B., 2016. Synergistic Use of Vis-NIR, MIR, and XRF Spectroscopy for the Determination of Soil Geochemistry. *Soil Sci. Soc. Am. J.* 80, 888–899. <https://doi.org/10.2136/sssaj2015.10.0361>
- Rossel, R.A.V., Walvoort, D.J.J., McBratney, A.B., Janik, L.J., Skjemstad, J.O., 2006. Visible, near infrared, mid infrared or combined diffuse reflectance spectroscopy for simultaneous assessment of various soil properties. *Geoderma* 131, 59–75. <https://doi.org/https://doi.org/10.1016/j.geoderma.2005.03.007>
- Shepherd, K.D., Walsh, M.G., 2002. Development of Reflectance Spectral Libraries for Characterization of Soil Properties. *Soil Sci. Soc. Am. J.* 66, 988–998. <https://doi.org/https://doi.org/10.2136/sssaj2002.9880>
- Stenberg, B., Rossel, R.A.V., Mouazen, A.M., Wetterlind, J., 2010. Chapter Five - Visible and Near Infrared Spectroscopy in Soil Science, in: Sparks, D.L. (Ed.), *Advances in Agronomy*. Academic Press, pp. 163–215.
- Tavares, T.R., Molin, J.P., Javadi, S.H., Carvalho, H.W., Mouazen, A.M., 2021. Combined Use of Vis-NIR and XRF Sensors for Tropical Soil Fertility Analysis: Assessing Different Data Fusion Approaches. *Sensors* . <https://doi.org/10.3390/s21010148>
- Xu, D., Chen, S., Viscarra Rossel, R.A., Biswas, A., Li, S., Zhou, Y., Shi, Z., 2019. X-ray fluorescence and visible near infrared sensor fusion for predicting soil chromium content. *Geoderma* 352, 61–69. <https://doi.org/https://doi.org/10.1016/j.geoderma.2019.05.036>